Supporting Information for
Environmental Science and Technology

Carbon, Hydrogen, and Nitrogen Isotope Fractionation Trends in *N*-Nitrosodimethylamine Reflect the Formation Pathway during Chloramination of Tertiary Amines

Stephanie Spahr[1,2], Urs von Gunten[1,2,3], and Thomas B. Hofstetter[*,1,3]

[1]Eawag, Swiss Federal Institute of Aquatic Science and Technology
[2]School of Architecture, Civil and Environmental Engineering (ENAC), Ecole Polytechnique Federale de Lausanne (EPFL)
[3]Institute of Biogeochemistry and Pollutant Dynamics (IBP), ETH Zürich

[*]Corresponding author: thomas.hofstetter@eawag.ch
phone +41 58 765 50 76, fax +41 58 765 50 28

14 Pages, 9 Figures, 3 Tables

Contents

S1 Safety considerations

N-Nitrosamines are mutagenic and probably carcinogenic to humans. Wear appropriate protective clothing, goggles, and gloves and work in a well-ventilated chemical fume hood. Keep away from heat, sparks, and flames.

S2 Chemicals

All chemicals were used without further purification. 5-(dimethylaminomethyl)furfuryl alcohol hydrochloride (DFUR, 96%) and *N,N*-dimethylthiophene-2-methylamine (DMTA) were purchased from ABCR and Santa Cruz Biotechnology, respectively. Ranitidine hydrochloride, *N,N*-dimethylbenzylamine (DMBA, 99%), *N*-nitrosodimethylamine (NDMA, 5000 μg/ml in methanol, 99.9%), 2-thiophenemethanol (98%), 2,2'-azino-bis(3-ethylbenzothiazoline-6-sulfonic acid) diammonium salt (ABTS, ≥98%), potassium iodide (≥99%), sodium nitrite ($NaNO_2$, 99%), sodium thiosulfate ($Na_2S_2O_3$, ≥98%), and potassium phosphate monobasic (KH_2PO_4, puriss, ≥99.5%) were purchased from Sigma Aldrich. Boric acid (>98%) was obtained from Fluka. For NH_2Cl preparation, we used sodium hypochlorite (6-14% HOCl, Sigma-Aldrich) and ammonium chloride (NH_4Cl, 99.5%, Fluka) or ^{15}N-enriched ammonium sulfate ($(NH_4)_2SO_4$, USGS26) that was purchased from the International Atomic Energy Agency (IAEA).[1]

Analyte stock solutions were made in ethyl acetate (99.7%, Chromasolv for HPLC, Sigma Aldrich), or methanol (99.99%, Fisher Scientific). These solvents were also used for solid phase extraction (SPE) in addition to pentane (99.0%, Sigma-Aldrich). Aqueous solutions were prepared with deionised water (18.1 MΩ · cm, Barnstead NANOpure Diamond Water Purification System). The pH value of buffered solutions was adjusted with sodium hydroxide pellets (NaOH, puriss, ≥99%, Sigma-Aldrich) or aqueous NaOH solution (Sigma-Aldrich). For SPME-GC/MS and SPME-GC/IRMS analyses the ionic strength of the samples was raised with sodium chloride (NaCl, 99.5%, Merck). Helium (He, 99.999%) was used as carrier gas for GC/MS and GC/IRMS analysis. Reference gases for GC/IRMS measurements were CO_2 (99.999%), N_2 (99.999%), H_2 (99.999%) and O_2 (99.999%) from Carbagas (Rümlang, Switzerland).

S3 Stable isotope analysis

S3.1 Reference isotope signatures

Table S1 C and N isotope signatures of in-house standards measured with elemental analyzer isotope ratio mass spectrometry (EA/IRMS).

Compound	δ^{15}N	δ^{13}C
ranitidine	–3.36 ± 0.11	–28.24 ± 0.03
DFUR	–2.22 ± 0.39	–19.76 ± 0.03
DMTA	–4.52 ± 0.08	–35.54 ± 0.03
NH_4Cl	–1.44 ± 0.03[a]	-
$(NH_4)_2SO_4$[b]	+53.7 ± 0.4[a]	-

[a] Reported as proxy for the initial δ^{15}N value of NH_2Cl generated from the reaction of HOCl with NH_4Cl or $(NH_4)_2SO_4$
[b] Standard reference material USG26 obtained from IAEA [1]

S3.2 Method quantification limits (MQLs) for C and N isotope analysis of DMTA

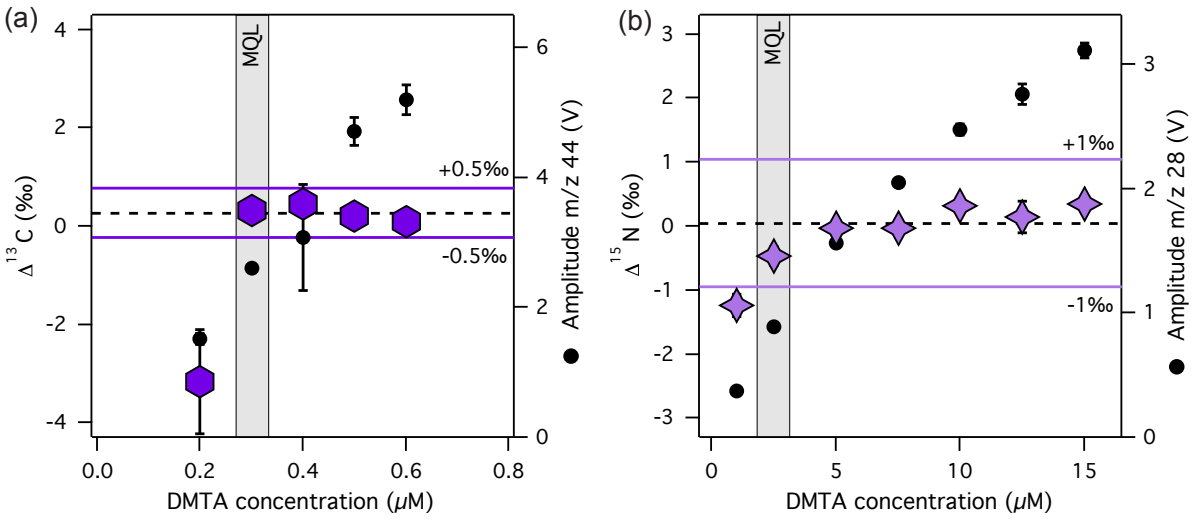

Figure S1 Accuracies of (a) C and (b) N isotope signatures of DMTA as function of the DMTA concentration. Amplitudes increased with increasing DMTA concentrations. MQLs were determined according to the moving mean procedure of Jochmann et al. [2] with intervals of ±0.5‰ and ±1‰ for C and N isotope analysis, respectively (purple lines). MQLs are indicated as grey bars and moving means by dashed lines.

S4 Isotope fractionation in tertiary amines during chloramination

S4.1 Isotope fractionation in DMTA and DMBA

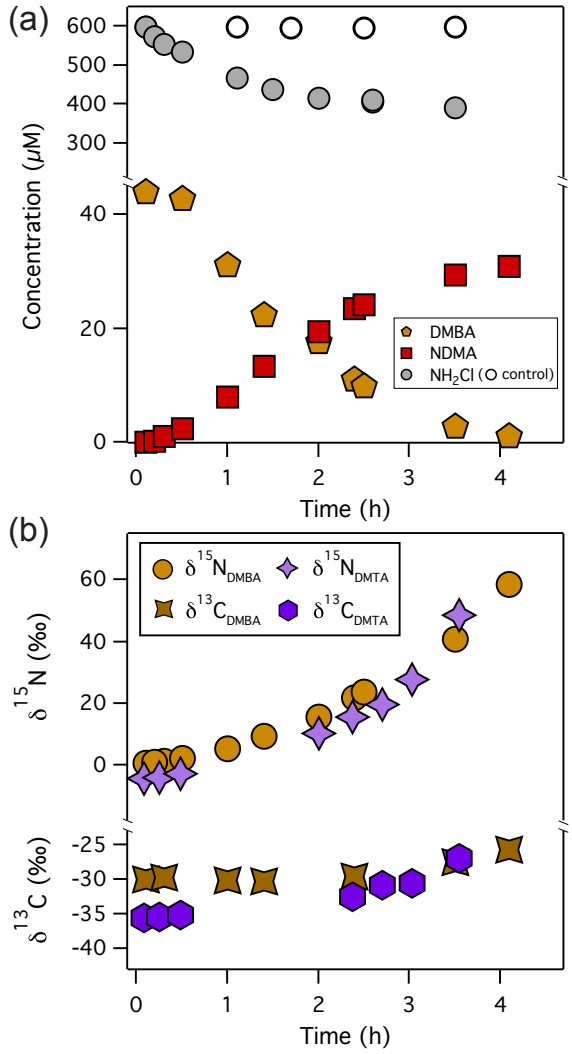

Figure S2 NDMA formation from the reaction of DMBA (40 μM) with NH_2Cl (600 μM) in 10 mM phosphate buffer at pH 8.0. Panel (a) shows DMBA degradation, NH_2Cl consumption, and NDMA formation over time. Panel (b) illustrates $\delta^{13}C$ and $\delta^{15}N$ values of DMBA (brown symbols) and DMTA (purple symbols) over time. Standard deviations of triplicate $\delta^{13}C$ and $\delta^{15}N$ measurements of DMTA and DMBA were $<0.4‰$ and $<0.8‰$, respectively, and smaller than the depicted symbols.

S4.2 Bulk isotope enrichment factors

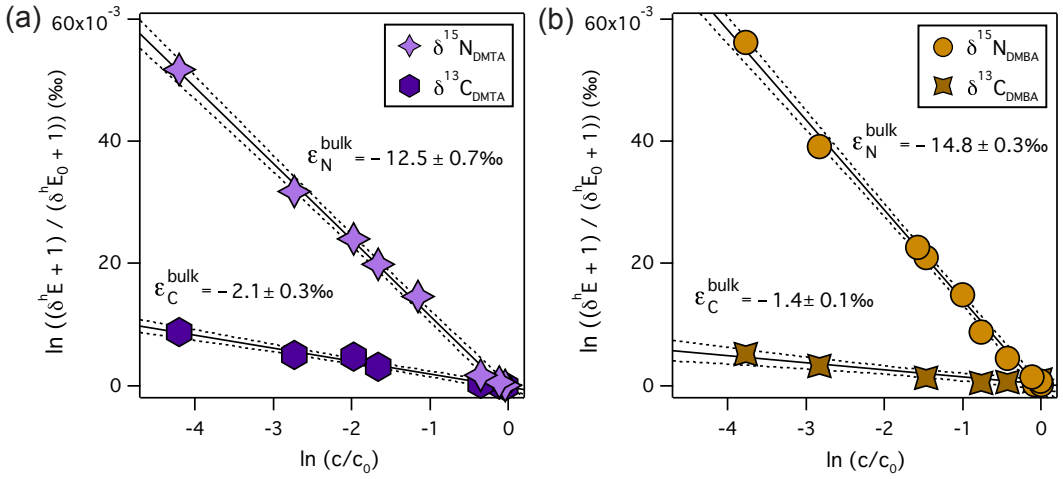

Figure S3 Linearized C and N isotope fractionation of (a) DMTA and (b) DMBA used to derive C and N bulk isotope enrichment factors, $\varepsilon_{\mathrm{C}}^{\mathrm{bulk}}$ and $\varepsilon_{\mathrm{N}}^{\mathrm{bulk}}$, respectively.

S4.3 ^{15}N equilibrium isotope effect associated with the deprotonation of DMTA

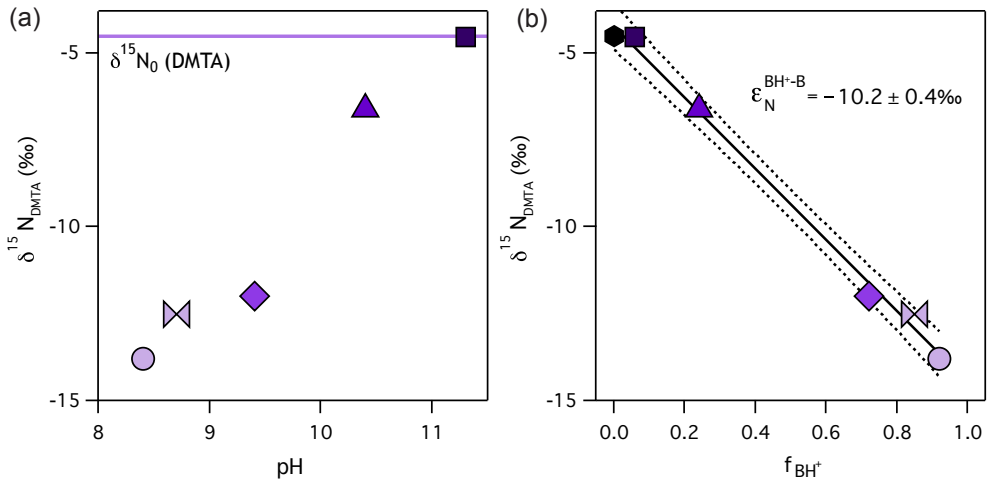

Figure S4 N isotope signatures ($\delta^{15}\mathrm{N}_{\mathrm{DMTA}}$) measured with SPME-GC/IRMS in the neutral fraction of DMTA (a) versus pH of the aqueous DMTA samples (from 8.4 - 11.3) in 10 mM phosphate buffer and (b) versus the fraction of protonated DMTA species ($\mathrm{f}_{\mathrm{BH^+}}$). The concentration of protonated DMTA in a sample was calculated using peak areas of the GC/IRMS measurements. The slope of the regression line corresponds to the enrichment factor for the deprotonation of DMTA ($\varepsilon_{\mathrm{N}}^{\mathrm{BH^+-B}}$). The standard deviation of triplicate $\delta^{15}\mathrm{N}_{\mathrm{DMTA}}$ measurements was <0.8‰ and smaller than the depicted symbols.

S4.4 Isotope enrichment factors and kinetic isotope effects associated with the reaction of DMTA and DMBA

The observable $AKIE_N$ is the weighted average of the protonated (f_{BH+}) and deprotonated fraction (1-f_{BH+}) of the tertiary amine and their respective isotope effects as shown in eq. S1.[4]

$$AKIE_N = f_{BH^+} \cdot EIE_N^{BH^+-B} \cdot AKIE_N^B + (1 - f_{BH^+}) \cdot AKIE_N^B \tag{S1}$$

The $AKIE_N^B$ that originates from the reaction of the deprotonated species is given by eq. S2. f_{BH+} at pH 8.0 was determined with eq. S3 using a pK_a of 9.75 ± 0.3 for DMTA (derived from SPME-GC/IRMS measurements) and a literature pK_a of 9.0 for DMBA.[3]

$$AKIE_N^B = \frac{AKIE_N}{(f_{BH^+} \cdot EIE_N^{BH^+-B}) + 1 - f_{BH^+}} \tag{S2}$$

$$f_{BH^+} = (1 + 10^{pH-pKa})^{-1} \tag{S3}$$

The deprotonation $EIE_N^{BH^+-B}$ was calculated with eq. S4, where the equilibrium isotope enrichment factor, $\varepsilon_N^{BH^+-B}$, was derived from the slope of the regression line of $\delta^{15}N$ versus f_{BH+} (see eq. S5 and Figure S4).[4]

$$EIE_N^{BH^+-B} = \frac{1}{1 + \varepsilon_N^{BH^+-B}} \tag{S4}$$

$$\delta^{15}N = \varepsilon_N^{BH^+-B} \cdot f_{BH^+} + \delta^{15}N_{ref} \tag{S5}$$

Table S2 Carbon and nitrogen bulk isotope enrichment factors, ε_C^{bulk} and ε_N^{bulk}, and apparent kinetic isotope effects, $AKIE_C$ and $AKIE_C$, for the chloramination of DMTA and DMBA. $EIE_N^{BH^+-B}$ is the equilibrium isotope effect associated with deprotonation of DMTA. $AKIE_N^B$ is the apparent kinetic isotope effect associated with the reaction of deprotonated DMTA and DMBA.

Compound	ε_C^{bulk} (‰)	ε_N^{bulk} (‰)	$AKIE_C$ (-)	$AKIE_N$ (-)	$EIE_N^{BH^+-B}$ (-)	$AKIE_N^B$ (-)
DMTA	–2.1±0.3	–12.5±0.7	1.0021±0.0003	1.0127±0.0007	1.0103±0.0004	1.0025±0.0011
DMBA	–1.4±0.1	–14.8±0.3	1.0014±0.0001	1.0150±0.0003	-[a]	1.0056±0.0007[b]

[a] not determined [b] calculated with the $EIE_N^{BH^+-B}$ of DMTA

S5 C, H, and N isotope ratios of NDMA during chloramination of four tertiary amines

Table S3 N isotope signatures of NDMA, $\delta^{15}N^{ini}_{NDMA}$ and $\delta^{15}N^{end}_{NDMA}$ in permil, determined at the beginning and the end of the reaction of ranitidine (3 μM), DFUR (3 μM), DMTA (40 μM), and DMBA (40 μM) with NH_2Cl which was added in 15-fold excess (45μM or 600 μM), respectively. All experiments were carried out in 10 mM phosphate buffer at pH 8.0. The molar NDMA yield corresponding to the $\delta^{15}N_{NDMA}$ values is specified in percent.

Precursor	$\delta^{15}\mathbf{N}^{ini}_{NDMA}$ (‰)	NDMA yield (%)	$\delta^{15}\mathbf{N}^{end}_{NDMA}$ (‰)	NDMA yield (%)	$\Delta^{15}\mathbf{N}_{NDMA}$ (‰)
ranitidine	–24.1	9	–3.5	97	+20.6
DFUR	–24.8	12	–8.7	65	+16.1
DMTA	–28.2	8	–19.8	75	+8.4
DMBA	–26.9	5	–13.2	58	+13.7

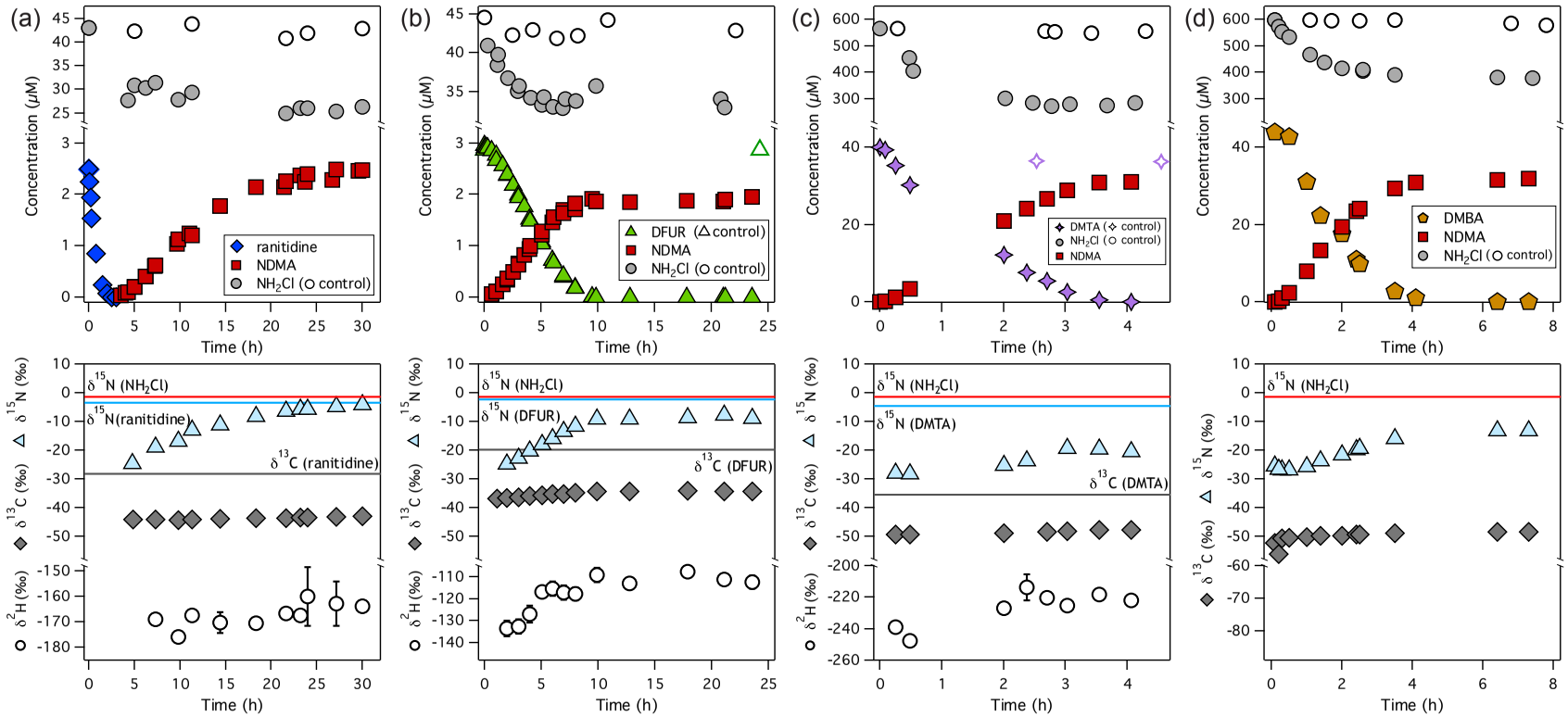

Figure S5 NDMA formation and corresponding C, H, and N isotope signatures of NDMA during the reaction of (a) ranitidine (3 μM), (b) DFUR (3 μM), (c) DMTA (40 μM), and (d) DMBA (40 μM) with NH_2Cl which was added in 15-fold excess (corresponding to concentrations of 45 μM and 600 μM NH_2Cl) in 10 mM phosphate buffer at pH 8.0. Upper panels show the degradation of the tertiary amine precursor as well as the disappearance of NH_2Cl and formation of NDMA. Lower panels show $\delta^{13}C$, $\delta^{2}H$, and $\delta^{15}N$ values of NDMA over time. Solid lines represent initial $\delta^{13}C$ and $\delta^{15}N$ values of the tertiary amine precursors and NH_2Cl. Note that we used the reference isotope signature of NH_4Cl (Table S1) as proxy for the initial $\delta^{15}N$ value of NH_2Cl. The initial C and N isotope signatures of DMBA were not determined. Standard deviations of triplicate $\delta^{13}C$, $\delta^{2}H$, and $\delta^{15}N$ measurements of NDMA were $<0.4‰$, $<11.5‰$, and $<0.5‰$, respectively, and mostly smaller than the depicted symbols.

S6 Impact of phosphate buffer concentration and buffer type on N isotope fractionation in NDMA

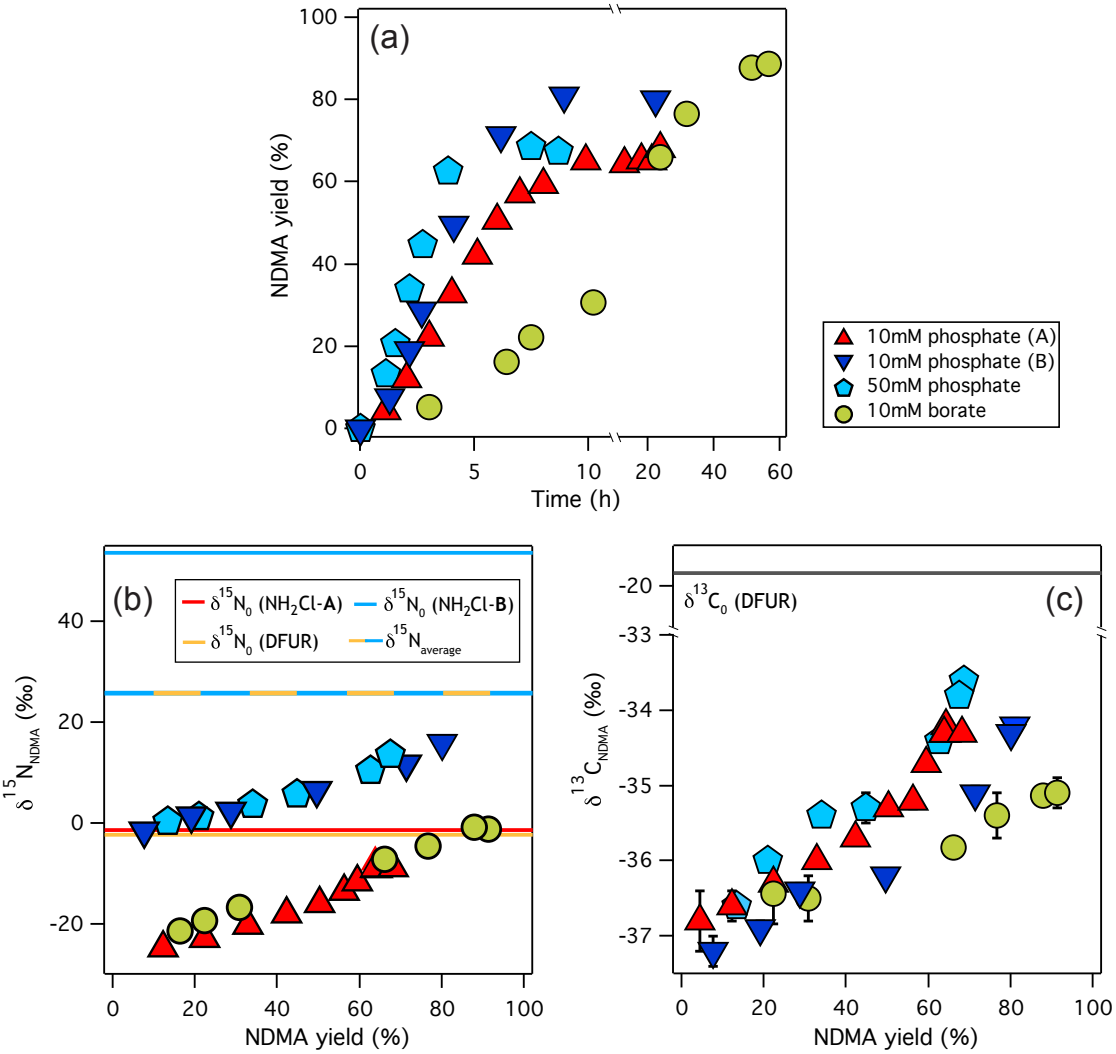

Figure S6 Panel (a) shows the NDMA yield in percent formed during the reaction of DFUR (3 μM) and NH_2Cl (45 μM) in 10 mM and 50 mM phosphate buffer and in 10 mM borate buffer at pH 8.0. Panels (b) and (c) show the corresponding δ^{15}N and δ^{13}C values of NDMA, respectively, versus the molar NDMA yield. Solid lines represent the initial isotope signatures of DFUR and NH_2Cl. Note that experiments in 10 mM phosphate buffer were conducted with NH_2Cl-**A** or NH_2Cl-**B** that had distinctly different initial δ^{15}N values (red vs. blue line in panel b). The experiment in 10 mM borate buffer was only conducted with NH_2Cl-**A**, the one in 50 mM phosphate buffer only with NH_2Cl-**B** what explains the shift in absolute δ^{15}N values of NDMA. The initial N isotope signature of NH_2Cl did not affect trends in N isotope signatures and δ^{13}C values of NDMA.

S7 Chloramination of 2-thiophenemethanol

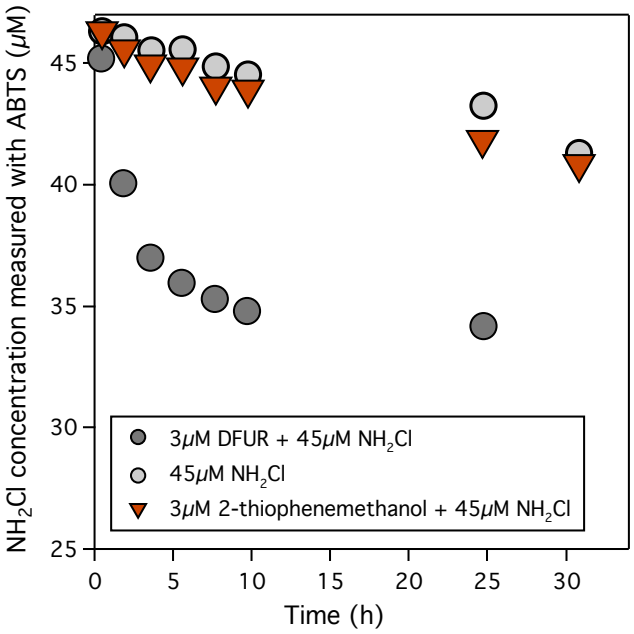

Figure S7 NH_2Cl concentration measured with the ABTS method over 30 h in three different batches containing (i) 3 μM DFUR and 45 μM NH_2Cl, (ii) 45 μM NH_2Cl, and (iii) 3 μM 2-thiophenemethanol and 45 μM NH_2Cl in 10 mM phosphate buffer at pH 8.0. Note that NH_2Cl concentrations were not corrected by the self-decay of chloramine observed in the NH_2Cl control.

S8 Impact of solution pH on isotope fractionation in NDMA

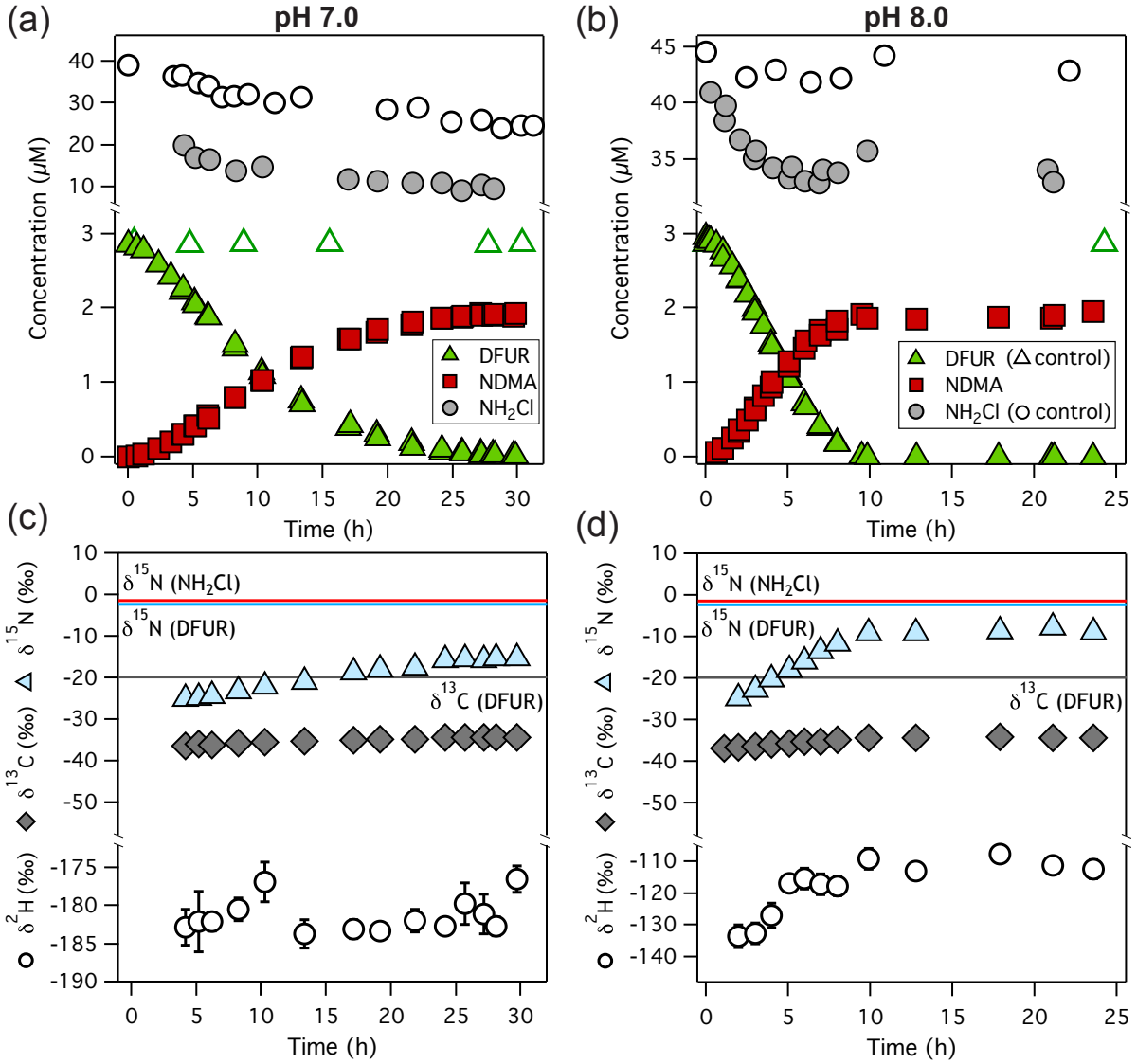

Figure S8 NDMA formation and corresponding C, H, and N isotope signatures of NDMA during the reaction of DFUR (3 μM) with NH_2Cl (45 μM) at pH 7.0 and pH 8.0 in 10 mM phosphate buffer. Upper panels (a) and (b) show the kinetics of DFUR and NH_2Cl degradation as well as NDMA formation at pH 7.0 and 8.0, respectively. Lower panels (c) and (d) show the corresponding $\delta^{13}C$, $\delta^{2}H$, and $\delta^{15}N$ values of NDMA over time. Solid lines represent the initial C and N isotope signatures of the precursor compounds DFUR and NH_2Cl. Note that we report the reference isotope signature of NH_4Cl (Table S1) as proxy for the initial $\delta^{15}N$ value of NH_2Cl. Standard deviations of triplicate $\delta^{13}C$, $\delta^{2}H$, and $\delta^{15}N$ measurements of NDMA were $<0.4‰$, $<4.0‰$, and $<0.3‰$, respectively, and mostly smaller than the depicted symbols.

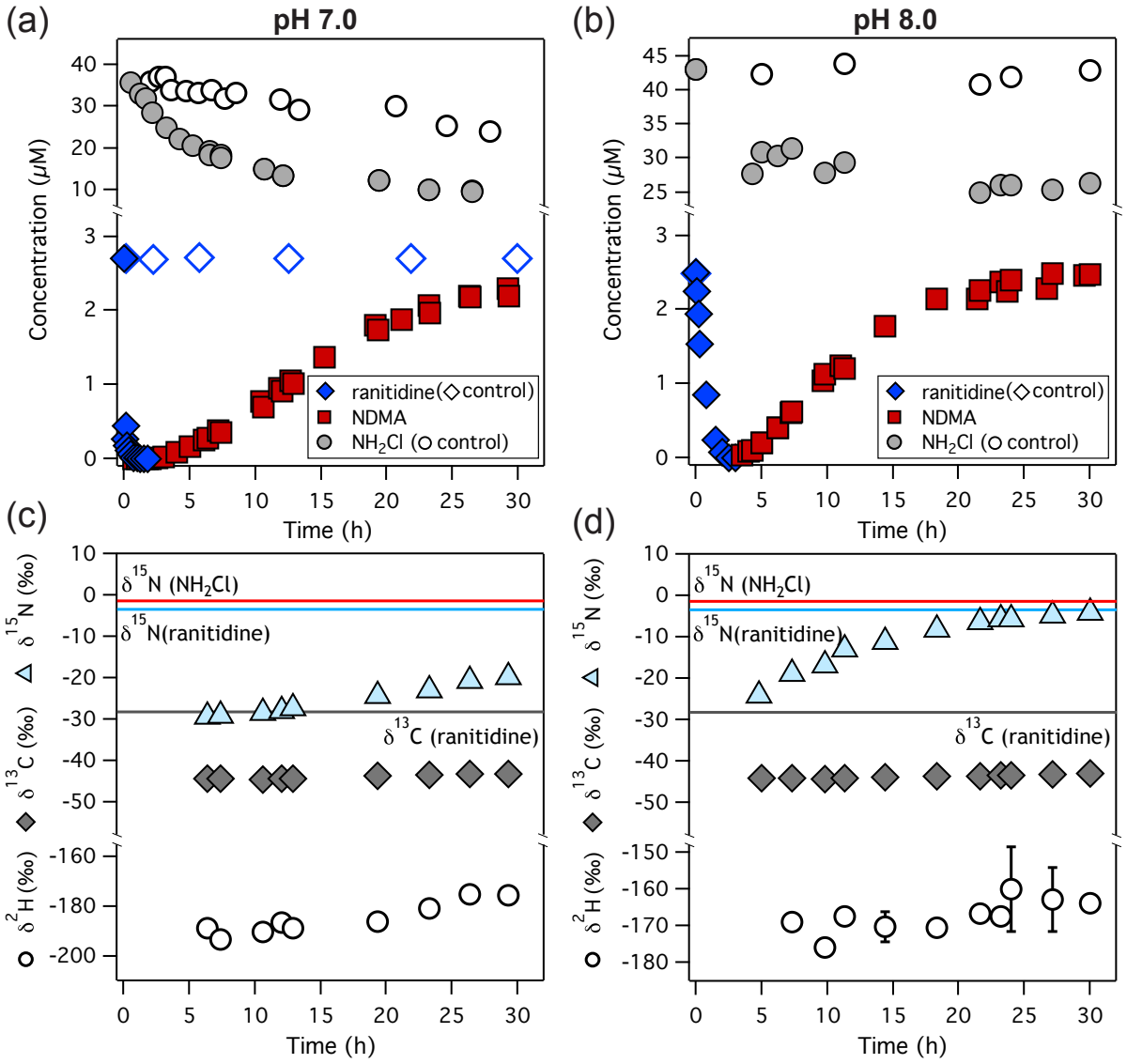

Figure S9 NDMA formation and corresponding C, H, and N isotope signatures of NDMA during the reaction of ranitidine (3 μM) with NH_2Cl (45 μM) at pH 7.0 and pH 8.0 in 10 mM phosphate buffer. Upper panels (a) and (b) show the kinetics of ranitidine and NH_2Cl degradation as well as NDMA formation at pH 7.0 and 8.0, respectively. Lower panels (c) and (d) show the corresponding $\delta^{13}C$, $\delta^{2}H$, and $\delta^{15}N$ values of NDMA over time. Solid lines represent the initial C and N isotope signatures of the precursor compounds ranitidine and NH_2Cl. Note that we report the reference isotope signature of NH_4Cl (Table S1) as proxy for the initial $\delta^{15}N$ value of NH_2Cl. Standard deviations of triplicate $\delta^{13}C$, $\delta^{2}H$, and $\delta^{15}N$ measurements of NDMA were $<0.3‰$, $<11.5‰$, and $<0.5‰$, respectively, and mostly smaller than the depicted symbols.

S9 References

[1] Böhlke, J. K., Gwinn, C. J., and Coplen, T. B. (1993). New reference materials for nitrogen-isotope-ratio measurements. *Geostandard Newslett.*, 17(1):159–164.

[2] Jochmann, M. A., Blessing, M., Haderlein, S. B., and Schmidt, T. C. (2006). A new approach to determine method detection limits for compound-specific isotope analysis of volatile organic compounds. *Rapid Commun. Mass Spectrom.*, 20(24):3639–3648.

[3] Rosenblatt, D. H., Hull, L. A., Luca, D. C. D., Davis, G. T., Weglein, R. C., and Williams, H. K. R. (1967). Oxidations of amines. II. Substituent effects in chlorine dioxide oxidations. *J. Am. Chem. Soc.*, 89(5):1158–1163.

[4] Skarpeli-Liati, M., Arnold, W. A., Turgeon, A., Cramer, C. J., and Hofstetter, T. B. (2011). pH-Dependent equilibrium isotope fractionation associated with compound-specific nitrogen and carbon isotope analysis by SPME-GC/IRMS. *Anal. Chem.*, 83(5):1641–1648.